Study of the effect of March 17-18, 2015 geomagnetic storm on the Indian longitudes using GPS and C/NOFS

Sarbani Ray[1], Bidyut Roy[1], Krishnendu Sekhar Paul[1], Samiddha Goswami[2], Christina Oikonomou[3], Haris Haralambous[4], Babita Chandel[5] and Ashik Paul[1]

[1]Institute of Radio Physics and Electronics, University of Calcutta, Calcutta, India

[2]S.K. Mitra Center for Research in Space Environment, University of Calcutta, Calcutta, India

[3]Frederick Research Centre, Cyprus

[4] Frederick University, Cyprus

[5]Department of Physics, Sri Sai University, Palampur, India

Key points: TEC enhancement observed associated with March 17-18, 2015 geomagnetic storm, intense scintillation observations beyond the northern crest of EIA, cycle slips and position deviations were recorded by GPS from Calcutta during the St. Patrick's day storm

Abstract

The largest geomagnetic storm in solar cycle 24 occurred during March 17-18, 2015 where the main phase of the storm commenced from 07:00 UT of March 17, 2015 and reached the Dst negative minimum at 22:00 UT. The present paper reports observations of TEC, amplitude and phase scintillations from different GPS stations of India during the storm of March 17 and highlights its effects on GPS. It also presents the global ESF occurrence during the storm using total ion density drift measurements from C/NOFS satellite. TEC enhancements were noted from stations along 77^{o}E meridian around 10:00 UT on March 17

This article has been accepted for publication and undergone full peer review but has not been through the copyediting, typesetting, pagination and proofreading process which may lead to differences between this version and the Version of Record. Please cite this article as doi: 10.1002/2016JA023127

compared to March 16 and 18 indicating positive storm effects arising out of equatorward neutral wind in the local morning-noon sector of the main phase. Intense scintillation observations from Calcutta were most extensive during 15:00-16:00 UT, March 17 and the receiver recorded a longitude deviation of 5.2 m during this time. Cycle slips of the order of 8 s could be observed during periods of intense phase scintillations on the same night. Intense scintillation observation from Palampur is an exceptional phenomenon attributed to the dramatic enhancement of the electric field due to PPEF leading to a very high upward ion velocity over the magnetic equator as recorded by C/NOFS. The total ion density measured globally by C/NOFS reveals two distinct longitude regions of ESF occurrence during the storm: i) East Pacific sector and ii) Indian longitude during the storm. The time and longitude of ESF occurrence could be predicted using the time of southward turning of IMF Bz.

Introduction

The most intense storm of solar cycle 24 was the storm of March 17-21, 2015, popularly known as the St. Patrick's Day storm. According to NOAA Scales (http://www.swpc.noaa.gov/noaa-scales-explanation) it was a severe (G4) storm as the Kp index reached 8- three times (12:00-15:00 UT, 15:00-18:00 UT, and 21:00-24:00 UT) on March 17. The main phase of the storm commenced from 08:00 UT of March 17, 2015 and reached the Dst negative minimum at 22:00 UT the same day. This level of geomagnetic disturbance has resulted in a variety of technological failures in the past, which include widespread voltage control problem in power grid systems, surface charging of spacecrafts and degradation of satellite-based navigation system performance for hours.

The first storm reported to have affected **G**lobal **P**ositioning **S**ystem (GPS) was the storm of October 22, 1999 [*Basu Su. et al.,* 2001] when the **W**ide **A**rea **A**ugmentation **S**ystem (WAAS) parameter **G**rid **I**onospheric **V**ertical **E**rror (GIVE) exceeded a value of 6 m**.** Later, during superstorms of October 29 and 30, 2003, November 20, 2003 and November 8, 2004 the **L**ocalizer **P**erformance with **V**ertical Guidance (LPV) service level of WAAS were unavailable for the entire WAAS coverage region for varying periods of time, with full or partial coverage loss in excess of 10 hours [*Doherty et al*., 2004; *Basu Su. et al*., 2008].

During a storm, a large polar cap dawn-dusk electric field promptly penetrates to equatorial latitudes until a shielding layer develops in timescales of about half an hour to several hours [*Kelley et al.*, 1979; *Fejer and Scherliess*, 1998; *Kikuchi et al*., 1996]. The **P**rompt **P**enetrating (under-shielded) **E**lectric **F**ield (PPEF) has eastward polarity on the dayside and westward polarity on the nightside respectively of the equatorial ionosphere. The PPEF of eastward polarity can cause large upward rise of the day- and evening-side ionosphere resulting in great increase of the **T**otal **E**lectron **C**ontent (TEC) as measured by GPS receivers [*Tsurutani et al*., 2004; *Maruyama et al.*, 2004; *Lin et al.*, 2005a, 2005b]. During such TEC storms the **E**quatorial **I**onization **A**nomaly (EIA) can expand poleward with the ionization crests moving into the midlatitudes [*Mannucci et al.*, 2005; *Abdu*, 1997]. In the dusk sector, the low latitude eastward PPEF is intensified [*Richmond et al.,* 2003; *Fejer and Scherliess,* 1998; *Abdu et al.*, 2007], when the **P**re-**R**eversal **E**nhancement (PRE) of zonal electric field arising from the *F* layer dynamo is present. Large uplift of the evening *F* layer to heights where recombination is negligible can cause instability growth by Rayleigh-Taylor mechanism leading to the generation of equatorial irregularities with scale sizes ranging from meters to hundreds of kilometers also known as **E**quatorial **S**pread ***F*** (ESF) [*Abdu et al.*, 2003; *Sastri et al*., 1997; *Basu et al.,* 2007], which cause scintillations of satellite signals [*Basu et al.,* 2010]. *Basu et al.,* [2010] showed the longitudinal confinement of VHF

scintillations and plasma depleted bubbles in the equatorial ionosphere, using **SCI**ntillation **N**etwork **D**ecision **A**id (SCINDA) network and **D**efense **M**eteorological **S**atellite **P**rogram (DMSP) satellite *in situ* measurements during the main phase of 30 large (rate of change of Dst $\leq$ -50 nTh^{-1} and minimum Dst $\leq$ -100 nT) magnetic storms in solar cycle 23. They also showed that from the knowledge of UT interval of the main phase of a storm, it is possible to determine the longitude interval over which bubbles and scintillations should be detected during the dusk sector of the storm main phase. *de Paula et al*., [2007] showed the local time influence of zonal magnetospheric electric field penetration to low latitudes on generation/inhibition of equatorial irregularities based on case studies of two geomagnetic storms. They showed that generation equatorial irregularities are suppressed when the main phase of the storm is in the daytime sector, when the disturbance dynamo electric field inhibits the pre-reversal electric field. ESF activity is enhanced when the main phase of the storm is in the dusk sector coinciding with the pre-reversal enhancement of the electric field. Recently, *Ray et al*., [2015] have shown from a study of 17 intense geomagnetic storms occurring during 1996-2005, that ESF occurs within four hours of IMF Bz crossing -10 nT in a longitude where the local time is dusk.

Depletions in ionization density and TEC have been reported earlier from the South American longitude sector during the magnetic storm of March 1989 [*Greenspan et al.*, 1991], July 2000 [*Basu et al.*, 2001, *Basu Su. et al.,* 2001] while large storm-enhanced density have been reported from the continental US during the magnetic storm of March 2001 [*Basu et al.*, 2005]. *Foster et al.* [2002] showed that during the large magnetic storm of March 31, 2001, plumes of greatly enhanced TEC were associated with the erosion of the outer plasmasphere by strong sub-auroral penetration electric fields. *Nava et al.,* [2016] studied the ionospheric response to the St. Patrick's Day storm in the middle and low-latitudes in the Asian, African, American, and Pacific longitude sectors using TEC

measurement. They have observed positive storm effects during the main phase of the storm depending on the longitude sector. During the recovery phase, strong decrease in ionization lasting for several days has been observed at all longitude sectors. For the same storm, *Astafyeva et al.* [2015] have observed dramatic TEC enhancements in different local time sectors and at different universal times, but around the same area of the Eastern Pacific region.

Under geomagnetically quiet conditions, *Bandyopadhyay et al.* [1997] first showed the effect of **C**arrier-to **No**ise Ratio (CNO) fluctuations or scintillations on standalone GPS **P**osition **D**ilution of **P**recision (PDOP) under sunspot number minimum condition. *DasGupta et al.,* [2004] showed that during high solar activity years, a position deviation of 11 m in latitude and 8 m in longitude corresponding to periods of intense scintillations has been observed. *Paul et al.* [2011] has reported occurrence of GPS phase scintillations and associated cycle slips observed during an unusually low solar activity period on October 8, 2009, perhaps for the first time from the Indian longitude sector. *Roy and Paul* [2013] discussed causative understanding behind occurrence of cycle slips on transionospheric satellite-based navigation systems from two stations on the anomaly crest region and beyond, during moderate to high solar activity levels of September 2011. *Das et al.,* [2014] illustrated the degradation of GPS positioning parameters during periods of scintillations under geomagnetic quiet conditions.

This paper presents a study of the ionospheric response using scintillation and TEC measurements to the St. Patrick's Day storm as observed from the Indian longitude sector. It highlights the impact of the storm on satellite-based navigation system in the Indian longitudes. This particular longitude sector is important because ESF has rarely been observed during geomagnetic storms from this longitude sector. *Ray et al*., [2015] reported from a study of seventeen intense geomagnetic storms occurring over nearly a solar cycle 1996-2005 that scintillations were observed during one storm only, the storm of February 11, 2004. Thus TEC and scintillation observations from Indian stations extending from the magnetic equator to the northern crest of the EIA and beyond during geomagnetic storm of March 17-18, 2015 becomes important as this provides a scope to study the impact of such storms on satellite-based navigation systems from this subcontinent.

Data

The present paper reports ionospheric TEC maps for Bangalore, Hyderabad, Lucknow and Palampur located along 77°E meridian, GPS CNO fluctuations or amplitude scintillations observed from Bangalore, Calcutta, Lucknow and Palampur, GPS cycle slips and position deviations from Calcutta, to understand impact of the storm from over the magnetic equator (Bangalore, Hyderabad) through the Equatorial Ionization Anomaly (EIA) crest region (Calcutta), just beyond the northern crest (Lucknow), and well beyond the northern crest (Palampur). The locations of the different stations are marked on a map of India shown in Figure 1. Zone of reception of satellite signals from these stations above an elevation of 15° are shown by the different colored ellipses. The magnetic equator and the position of typical northern crest of the EIA are also indicated in this figure. This paper also presents a global response of ESF during the March 17 storm observed from *in situ* ion density measurement during dusk sector.

Two-dimensional ionospheric maps of TEC have been generated, measured from a chain of four GPS receivers extending from the magnetic equator to locations beyond the northern crest of the EIA. Ionospheric TEC data are available from the **I**nternational **G**NSS **S**ervice (IGS) stations at Bangalore (13.02°N, 77.5°E geographic; magnetic dip: 11.78°N), Hyderabad (17.41°N, 78.55°E geographic; magnetic dip: 21.69°N) and Lucknow (26.91°N, 80.95°E geographic; magnetic dip: 39.75°N) at a sampling interval of 1 minute. This data has been combined with corresponding GPS TEC data measured at Palampur (32.11°N, 76.53°E geographic; magnetic dip: 48.34°N) measured at 1 minute sampling to generate Slant TEC contours as a function of subionospheric latitude and longitude every 2 hours during March 16-22, 2015. Slant TEC has been used instead of Vertical TEC as the sharp spatial gradients of ionization existing in the equatorial region makes simple geometric conversion inappropriate. *Paul et al.* [2005] highlights this fact using TEC recorded at Calcutta during 1977-1990. *Paul et al.* [2011] studied the importance of sharp spatial gradients of ionization occurring in the Indian longitude sector using GPS TEC recorded from a chain of GAGAN stations.

GPS amplitude scintillation index S4 measured on different satellite vehicle links at 1 minute sampling interval from Bangalore, Lucknow and Palampur have been used to study occurrence of scintillations, if any, at these stations during the magnetic storm. The station at the Institute of Radio Physics and Electronics (IRPE), University of Calcutta, Calcutta (22.58°N, 88.38°E geographic; magnetic dip: 32°N) is part of the international SCINDA program of the US Air Force. Data recorded under this program are available at http://capricorn.bc.edu/scinda/india. GPS CNO fluctuations and S4 at L1 frequency have been measured from Calcutta at sampling rates of 1s and 1 minute respectively to understand amplitude scintillation occurrences, if any, from Calcutta. CNO deviations have been

calculated with a 10 minute moving average period to limit spatial variations in CNO arising out of the movement of the satellite vehicle.

GPS phase measurements at 50Hz sampling from Calcutta have been detrended to extract the ionospheric contribution from the path length and Doppler effects. The second difference of the measured phase removes contributions of the path length and Doppler and extracts the ionospheric component. This data has been used to estimate cycle slips leading to loss of lock of signal by the receiver. Position deviations of the GPS receiver have been measured at Calcutta in terms of latitude and longitude, sampled at 1 s, to understand effect of the magnetic storm on navigation accuracy. Deviations have been calculated taking the reference at 00:00 UT (=06:00 LT at Calcutta), when ionospheric effects are minimum. For all the GPS TEC and scintillation data analyses, an elevation mask of 15° has been maintained in order to eliminate the multipath effects.

The Communication and Navigation Outage Forecast System (C/NOFS) satellite, a US Air Force mission to forecast ambient plasma densities and irregularities in the equatorial ionosphere [de La Beaujardière et al., 2004], was launched in April 2008 into a 13^{o} inclination elliptical orbit having perigee of 400 km and apogee of 850 km. The Coupled Ion Neutral Dynamics Investigation (CINDI) is a NASA sponsored mission conducted by the University of Texas at Dallas (UTD) to enhance the science objectives of C/NOFS. Instruments on C/NOFS satellite measure total ion density, ion drift velocity, ion temperature, and the constituent ion composition at 0.5 s interval or every 4 km along the satellite track [*Stoneback et al.,* 2013]. The tracks of C/NOFS satellites that exhibited fluctuations in total ion density and intercepted the Indian longitude sector have been shown with different shades of green in Figure 1. The portions of the tracks with fluctuations have been marked with red.

Interplanetary magnetic field (IMF) Bz data at 64 s sampling interval have been obtained from the Advanced Composition Explorer (ACE) satellite (http://www.srl.caltech.edu/ACE/). Dst index for the storm has been obtained from World Data Center (http://wdc.kugi.kyoto-u.ac.jp).

Results and Discussions

The most intense storm of solar cycle 24 occurred on March 17, 2015 when a high-speed CME hit Earth's magnetosphere. At first, the CME's impact just produced a minor G1-class (Kp = 5) magnetic disturbance. As the Earth moved into the CME's strongly-magnetized wake, the storm intensified and became a G4-class (Kp = 8) event. The initial phase started at 03:00 UT 4 hours after which the main phase started at 07:00 UT [Figure 2(a)]. At 09:00 UT a small minimum in Dst of -73 nT was observed followed by a short recovery for 3 hours after which Dst started decreasing steadily. For 19 hours, from 15:00 UT, March 17 to 10:00 UT, March 18, Dst remained below -100 nT, with a minimum hourly Dst value of -223 nT at 22:00 UT, March 17. The IMF Bz [Figure 2(b)] turned southward and crossed -10 nT at 07:41 UT on March 17 and stayed below -10 nT for 41 minutes. Then after several northward turnings Bz crossed -10 nT at 11:50 UT and was below -10nT for another 42 minutes. The peak southward IMF Bz of -28.26 nT was observed at 13:26 UT after which there was an interval of 3 hours 45 minutes, from 13:40 to 17:25 UT, when Bz remained continuously below -10 nT. Finally, from 18:23 UT to 23:08 UT, for 4 hours 45 minutes, Bz remained below -10 nT before restoring to its ambient value.

(i) TEC Enhancement

Daytime TEC from the Indian longitude sector could provide an idea of the impact of the storm on the equatorial and low latitudes. TEC measured from the stations Bangalore, Hyderabad, Lucknow and Palampur, located along 77°E longitude have been combined and plotted every 2 hours during March 16-22, 2015 above an elevation mask of 15^{o}. Figures 3(a), (b) and (c) show the result at 10:00 UT for March 16, 17 and 18, 2015 respectively. Significant enhancement in the maximum value of STEC could be noted at 10:00 UT from 120 TECU on March 16, 2015 to 210 TECU on March 17, 2015. At 10:00 UT (IST=UT + 05:30), which corresponds closely to the time of diurnal maximum in the Indian longitude sector, Slant TEC maximum is found around 24°N, 75°E geographic. A secondary maximum is noted around 23°N, 85°E. The latitudinal gradients of TEC are also very sharp on March 17, 2015 between subionospheric latitude range of 23°-28°N, compared to March 16 and 18, 2015. Maximum STEC values were reduced to levels of 120 TECU again on March 18, 2015. It is important to note that the daily sunspot number for March 16, 17 and 18, 2015 were 46, 38 and 41 respectively.

Prolls et al., [1991] have explained the positive storm effects in terms of increase in ionization density particularly in the noon-afternoon sector as arising out of sudden uplifting of the *F*-layer, which propagates from the polar latitudes to lower latitudes with velocity of the order of hundred meters per second. This propagation is associated with the large-scale traveling atmospheric ionospheric disturbances (TAIDs). *Balan et al*., [2010] proposed a physical mechanism for positive storms at low and mid-latitudes with multi-instrument observations, theoretical modeling, and basic principles. According to this mechanism, an equatorward neutral wind is required to produce positive ionospheric storm as the mechanical effects of the wind reduces downward diffusion of plasma along the field lines and lifts the

ionosphere to high altitudes where chemical loss is less resulting in accumulation of plasma at ionospheric peak at about ±30^{o} magnetic dip. The positive ionospheric storm occur mostly in the longitude sector where the onset of geomagnetic storm falls in the ionization production dominated morning-noon local time sector when the plasma accumulation due to the mechanical effect of the wind is much greater than the plasma loss due to its chemical effect. Thus the onset of the St. Patrick's Day storm at 03:00 UT corresponded to morning 08:08 LT at 77^{o}E longitude where positive storm effect was observed.

(ii) Scintillation Observations and Impact on GPS

Next, occurrence of ionospheric scintillations in amplitude and phase were studied during the post-sunset hours from these stations located from the magnetic equator to well beyond the northern crest of the EIA. On March 17, 2015, a number of GPS satellite links, namely, SV6, 10, 20 and 28 experiencing amplitude scintillations with S4 in excess of 0.6 were observed from Calcutta during 14:00-17:00 UT (20:00-23:00 LT). However, there were no such phenomena on March 16 and 18, 2015. Figure 4 shows (a) CNO deviations for scintillations observed from Calcutta on SV10, (b) S4, (c) second difference of phase and (d) satellite elevation angle variations during 16:30-20:45 UT of March 17, 2015. One prominent patch of intense scintillation could be identified from the CNO, S4 and phase during 16:42-17:22 UT. Maximum S4 value on SV10 link was 0.7 recorded at 16:51 UT. Figure 5 shows the second difference of the recorded phase on the GPS SV10 L1 signal over a brief interval 16:15-16:16 UT to show occurrence of cycle slips. Discontinuities in phase of duration 8 s could be found after 16:15:31 UT on the SV10 link indicating occurrence of cycle slips. Figure 6 presents the statistics of cycle slips of different durations which occurred at Calcutta on March 17, 2015. It is noted that majority of the cycle slips are of duration less than 8 s, but there were 7 cases when cycle slip duration exceeded 6 s. It is important to note that signal-in-space (SIS) performance requirement for APV approach specified by the International

Civil Aviation Organization (ICAO) stipulates a Time-to-Alert (TTA) of 10 s for APV I and 6 s for APV II operations [*ICAO*, 2006].

Paul et al. [2011] has reported occurrence of GPS phase scintillations and associated cycle slips observed during an unusually low solar activity period on October 8, 2009, for the first time from the Indian longitude sector. *Roy and Paul* [2013] discussed causative understanding behind occurrence of cycle slips on transionospheric satellite-based navigation systems from two stations on the anomaly crest region and beyond, during moderate to high solar activity levels of September 2011. The basic motivation behind showing the phase scintillation patches in Figure 4 followed by a representative sample of cycle slip observed and the overall statistics of the same was to highlight the impact of the storm on navigation system. It is important to note that there is no phase scintillation report available from the Indian longitude sector associated with the March 17-18, 2015 geomagnetic storm. Cycle slip durations of 8 s were noted during 16:15-16:16 UT from Calcutta which is in excess of 6 s specified by the International Civil Aviation Organization (ICAO) has serious implications for satellite-based navigation systems.

Figure 7 compares the occurrence of scintillation on different GPS tracks observed from Calcutta for each hour of 14:00-17:00 UT of March 17, 2015 [Figure 7(b)] with the corresponding hours of March 16 [Figure 7(a)] and March 18 [Figure 7(c)]. The GPS tracks are plotted in terms of subionospheric latitude and longitude and color indexed for different S4 levels. The green portion of the tracks represent no scintillation ($S4 \leq 0.2$), the blue portion mild scintillations ($0.2 < S4 \leq 0.4$), the pink portion moderate scintillation ($0.4 < S4 \leq 0.6$) and the red portion intense scintillations ($S4 > 0.6$). The occurrence of scintillations during local premidnight hours 14:00–17:00 UT corresponds to the second main phase of the storm from 12:00 to 22:00 UT which is the dusk to dawn sector for

Calcutta (LT = UT+6h). Also, the onset of scintillations followed the time of southward turning of IMF Bz and crossing -10 nT for the second time at 11:50 UT. *Ray et al.*, [2015] reported from a study of 17 intense geomagnetic storms that ESF has been found to occur within 4 hours after the southward Bz crossed -10 nT at a longitude where dusk time prevailed. In case of the St. Patrick's Day Storm, scintillations occurred after 2 hours 10minutes subsequent to the time of southward Bz crossing -10 nT. Large (< -10 nT) southward components of Bz for a considerable period of time (30 minutes to 3hours) strengthens the solar wind-magnetospheric dynamo [*Gonzalez et al*., 1994] thus producing rapid changes in the cross polar cap potentials and undershielding by the region 1 current to allow the penetration of the high latitude electric field to the low latitude ionosphere.

In order to study the position accuracy of GPS during this storm, position deviations of the receiver have been measured at Calcutta every hour during 13:00-22:00 UT of March 16-18, 2015. The position deviations, expressed in terms of latitude and longitude in metres, have been calculated taking the reference at 00:00 UT. During 15:00-16:00 UT on March 17, a maximum deviation of 5.2 m in longitude was observed which is much larger than the 2 m longitude deviation measured on March 16 and 18 [Figure 8]. However, during the same hour, the maximum latitude deviation of 2.1 m is comparable to the 2-3 m values observed on March 16 and 18. The time 15:00–16:00 UT when maximum position deviation was observed corresponded to the hour when two GPS links were experiencing moderate to intense scintillations [Figure 7(b), middle frame]. Intense (S4 > 0.6 corresponding to **S**cintillation **I**ndex (SI) > 15dB) scintillations gives rise to signal fades of the order of 12 dB [*Ray et al*., 2003]. If the signal fade exceeds the fade margin of the receiver the satellite link may become unusable for navigation thereby deteriorating the performance of the GPS receiver [*DasGupta et al.,* 2004].

Scintillation measurements from stations along 77°E were examined throughout the storm period, for Bangalore near the magnetic equator, Lucknow just beyond the anomaly crest and Palampur well beyond the crest. No scintillations were observed from Bangalore and Lucknow throughout the storm period i.e. March 16-21. Surprisingly from Palampur located well beyond the anomaly crest, intense scintillations were observed on three links during 14:00-17:00 UT (19:00-22:00 LT) on March 17, while no scintillations were observed on March 16 and 18. Figure 9, similar to Figure 7, presents a comparison of scintillation occurrence at Palampur on March 16, 17 and 18.

The global ESF response of the ionosphere to the St. Patrick's Day storm has been studied with total ion density (Ni) and vertical drift velocity measurements (Vz) from C/NOFS satellites during the local dusk sector. Figure 10 shows the variation of these two parameters with longitude observed on March 17. During the whole storm period of March 16-21, 2015, moderate fluctuations in ion density were observed on March 17, in the time interval 08:45-08:51 UT in the longitude interval 154.24°E-174.94°E [Figure 10(a)], intense fluctuations were observed during 10:17-10:32 UT in the longitude interval 127.65°E - 184.24°E [Figure 10(b)], and mild fluctuations during 11:59-12:13 UT in the longitude sector 134.40°E-187.93°E [Figure 10(c)]. At a later time, during 16:35-16:47 UT, intense fluctuations were observed in the longitude interval 53.88°E-97.44°E [Figure 10(d)]. Corresponding to the patches of intense density, amplitude of fluctuations of the order of 2.5×10^6 m^{-3} and 2×10^6 m^{-3} respectively [Figures 10 (b) and (d)], maximum vertical plasma drift velocity were observed to be 123 ms^{-1} at 157.17°E longitude and 150 ms^{-1} at 85.24°E.

The high vertical plasma drift measured by C/NOFS at the equator in the Indian longitude sector accounts for the scintillation observations at Palampur (48° magnetic dip) located far beyond the normal anomaly crest location (±30° magnetic dip). The intensified eastward PPEF at dusk superimposed on the normal low latitude zonal eastward electric field

gave rise to a strong upward **E×B** drift raising the *F* layer to great heights where conditions favourable for generation of irregularities through instability mechanism exist. The irregularities then diffused down the field lines to ionospheric heights at off-equatorial locations like Palampur.

Density fluctuations observed in the East Pacific longitude sector [Figure 10(a), (b) and (c)] commenced at 08:45 UT, 1h 04min after southward Bz exceeded -10 nT at 07:41 UT. The corresponding local time at the first longitude encountering ESF 154.24^{o}E is 19:02 in the dusk sector. The fluctuations then intensified during 10:17-10:32 UT [Figure 10(b)] and became mild during 11:59-12:13 UT [Figure 10(c)]. For the fluctuations in the Indian longitude sector [Figure 10(d)], the commencement at 16:35 UT was 2hours 55minutes after the time of Bz crossing -10 nT at 13:40 UT. The local time at the first longitude encountering ESF 53.88^{o}E was 20:11. A world map showing the longitude of ESF occurrence arising out of PPE indexed with the corresponding time of Bz crossing -10 nT for 17 intense storms was presented in Figure 12 of *Ray et al*., [2015]. The cases of ESF observed in the East Pacific sector and Indian longitude corroborates the observations.

Conclusions

The ionospheric response to the St. Patrick's Day Storm as observed in the Indian longitude sector has been presented. It is observed that the storm consisted of two components: one moderate storm of short duration with minimum Dst ~ -73 nT and an intense storm of minimum Dst ~ -223 nT. Corresponding to the two storms there were two main phases and two prominent southward turnings of IMF Bz. ESF have been observed in response to PPEF during the two main phases and subsequent to corresponding southward turning of IMF Bz at two longitude sectors where dusk condition prevailed: first one at the East Pacific sector and the second one at the Indian longitude sector. The times of

occurrence were within 3 hours of time of southward turning of Bz for both the occurrences. It is conclusive that the time of southward turning of IMF Bz can be used to predict the time and longitude of ESF occurrence as proposed by *Ray et al*., [2015].

Positive storm effects were observed in the Indian longitude sector in response to the St. Patrick's Day storm. These were caused by an equatorward neutral wind. This is indicated from the fact that the onset of the storm was in the ionization production dominated local morning to noon sector for this longitude zone when plasma accumulation due to mechanical effect of the wind is greater than the chemical loss.

The unacceptable position deviations observed corresponding to amplitude scintillation observations on March 17 at Calcutta and cycle slips observed during phase scintillations on the same night show clearly the degradation of GPS receiver performance when subject to a storm of such severity. The degradation of GPS receiver performance implies its measurements become unreliable under intense geomagnetic storm conditions. Observations from the Indian longitude sector on the impact of severe geomagnetic storms on satellite based navigation system have not been reported to date.

Acknowledgements

C/NOFS CINDI data are provided through the auspices of the CINDI team at the University of Texas at Dallas (http://cindispace.utdallas.edu). IGS data are available from the website http://sopac.ucsd.edu. The SCINDA data for Calcutta is available at http://capricorn.bc.edu/scinda/india. GPS data recorded at Palampur is available with the corresponding author, Prof. A. Paul. One of the authors (Samiddha Goswami) acknowledges the support provided by the Department of Science and Technology (DST), Govt. of India in the form of Research Fellowship. Two of the authors (Sarbani Ray and Ashik Paul)

acknowledge the support provided through scholarship under the Erasmus Mundas Leaders program of the European Union at Frederick University, Cyprus.

References

Abdu, M. A. (1997), Major phenomena of the equatorial ionospherethermosphere system under disturbed conditions, *J. Atmos. Sol. Terr. Phys.*, 59, 1505–1519.

Abdu, M. A., I. S. Batista, H. Takahashi, J. MacDougall, J. H. Sobral, A. F. Medeiros, and N. B. Trivedi (2003), Magnetospheric disturbance induced equatorial plasma bubble development and dynamics: A case study in Brazilian sector, *J. Geophys. Res.*, 108(A12), 1449, doi:10.1029/
2002JA009721.

Abdu, M. A., T. Maruyama, I. S. Batista, S. Saito, and M. Nakamura (2007), Ionospheric responses to the October 2003 superstorm: Longitude/local time effects over equatorial-low and mid-latitudes, *J. Geophys. Res.*, 112, A10306, doi:10.1029/2006JA012228.

Astafyeva, E., I. Zakharenkova, and M. Förster (2015), Ionospheric response to the 2015 St. Patrick's Day storm: A global multi-instrumental overview, *J. Geophys. Res. Space Physics*, 120, 9023–9037, doi:10.1002/2015JA021629.

Balan, N., K. Shiokawa, Y. Otsuka, T. Kikuchi, D. Vijaya Lekshmi, S. Kawamura, M. Yamamoto, and G. J. Bailey (2010), A physical mechanism of positive ionospheric storms at low latitudes and midlatitudes, *J. Geophys. Res.*, 115, A02304, doi:10.1029/2009JA014515.

Bandyopadhyay, T., A. Guha, A. DasGupta, P. Banerjee, and A.Bose (1997), Degradation of navigational accuracy with Global Positioning System during periods of scintillation at equatorial latitudes, *Electronics Lett., 33*(12), 1010-1011.

Basu, S., Su. Basu, K.M. Groves, H.C. Yeh, S.Y. Su, F.J. Rich, P.J.S. Sultan and M.J. Keskinen (2001), Response of the equatorial ionosphere in the South Atlantic region to the great magnetic storm of July 15, 2000, *Geophys. Res. Letts.*, 28, 18, 3577-3580.

Basu, S., Su. Basu, K. M. Groves, E. MacKenzie, M. J. Keskinen, and F. J. Rich (2005), Near-simultaneous plasma structuring in the midlatitude and equatorial ionosphere during magnetic superstorms, *Geophys. Res. Lett.*, 32, L12S05, doi:10.1029/2004GL021678.

Basu, S., Su. Basu, F. J. Rich, K. M. Groves, E. Mackenzie, C. Coker, Y. Sahai, P. R. Fagundes, and F. Becker-Guedes (2007), Response of the equatorial ionosphere at dusk to penetration electric fields during intense magnetic storms, *J. Geophys. Res.*, 112, A08308, doi:10.1029/2006JA012192.

Basu, S., S. Basu, E. MacKenzie, C. Bridgwood, C. E. Valladares, K. M. Groves, and C. Carrano (2010), Specification of the occurrence of equatorial ionospheric scintillations during the main phase of large magnetic storms within solar cycle 23, *Radio Sci.*, 45, RS5009, doi:10.1029/2009RS004343.

Basu, Su., et al. (2001), Ionospheric effects of major magnetic storms during the International Space Weather Period of September and October 1999: GPS observations, VHF/UHF scintillations, and in situ density structures at middle and equatorial latitudes, *J. Geophys. Res.*, 106, 30,389.

Basu, Su. et al. (2008), Large magnetic storm-induced nighttime ionospheric flows at midlatitudes and their impacts on GPS-based navigation systems, *J. Geophys. Res.*, 113, A00A06, doi:10.1029/2008JA013076

Das, T., B. Roy, and A. Paul, (2014), Effects of transionospheric signal decorrelation on Global Navigation Satellite System (GNSS) performance studied from irregularity dynamics around the northern crest of EIA, *Radio Sci., 49,* doi: 10.1002/2014RS005406.

DasGupta, A., S. Ray, A. Paul, P. Banerjee, and A. Bose (2004), Errors in position-fixing by GPS in an environment of strong equatorial scintillations in the Indian zone, *Radio Sci.*, *39*(RS1S30), doi:10.1029/2002RS002822.

de La Beaujardière ~~Beaujardie`re,~~ O., et al. (2004), C/NOFS: A mission to forecast scintillations, *J. Atmos. Sol. Terr. Phys*., 66, 1573– 1591, doi:10.1016/j.jastp.2004.07.030

de Paula E.R. et al. (2007), Characteristics of *F*-region plasma irregularities over Brazilian longitudinal sector, *Ind. J. Radio & Space Physics 36*(August), 268-277.

Doherty, P., A. J. Coster, and W. Murtagh (2004), Eye on the ionosphere: Space weather effects of October-November 2003, *GPS Solutions*, 8,267– 271, doi:10.1007/s10291-004-0109-3.

Fejer, B. G., and L. Scherliess (1998), Mid- and low-latitude prompt penetration ionospheric plasma drifts, *Geophys. Res. Lett.*, 25(16), 3071– 3074.

Foster, J. C., P. J. Erickson, A. J. Coster, J. Goldstein, and F. J. Rich (2002), Ionospheric signatures of plasmaspheric tails, *Geophys. Res. Lett.*, 29(13), 1623, doi:10.1029/2002GL015067.

Gonzalez, W. D., J. A. Joselyn, Y. Kamide, H. W. Kroehl, G. Rosoker, B. T. Tsuruani, and V. M. Vasyliunas (1994), What is a geomagnetic storm?, *J. Geophys. Res*., 99(A4), 5771–5792, doi:10.1029/93JA02867.

Greenspan, M.E. C.E. Rasmussen, W.J. Burke and M.A. Abdu (1991), Equatorial density depletions observed at 840km during the great magnetic storm of March 1989, *J. Geophys. Res.*, 96, 13931

International Civil Aviation Organization, ICAO (2006), Standard and Recommended Procedures (SARPS), Annex 10, Aeronautical Telecommunication, Radio Navigation Aids, vol. I, 6th ed.

Kelley, M. C., B. G. Fejer, and C. A. Gonzales (1979), An explanation for anomalous ionospheric electric fields associated with a northward turning of the interplanetary magnetic field, *Geophys. Res. Lett.*, 6(4), 301– 304.

Kikuchi, T., H. Lu¨hr, T. Kitamura, O. Saka, and K. Schlegel (1996), Direct penetration of the polar electric field to the equator during DP2 event as detected by the auroral and equatorial magnetometer chains and the EISCAT radar, *J. Geophys. Res.*, 101(A8), 17,161–17,174.

Lin, C. H., A. D. Richmond, J. Y. Liu, H. C. Yeh, L. J. Paxton, G. Lu, H. F. Tsai, and S.-Y. Su (2005a), Large-scale variations of the low latitude ionosphere during the October–November 2003 superstorm: Observational results, *J. Geophys. Res.*, 110, A09S28, doi:10.1029/2004JA010900.

Lin, C. H., et al. (2005b), Theoretical study of the low- and midlatitude ionospheric electron density enhancement during the October 2003 superstorm: Relative importance of the neutral wind and the electric field, *J. Geophys. Res.*, 110, A12312, doi:10.1029/2005JA011304.

Mannucci, A. J., B. T. Tsurutani, B. A. Ijima, A. Komjathy, A. Saito, W. D. Gonzalez, F. L. Guarnieri, U. J. Kozyra, and R. Skoug (2005), Dayside global ionospheric response to the major interplanetary events of October 29 – 30, 2003 ‘‘Halloween Storm’’, *Geophys. Res. Lett.*, 32, L12S02, doi:10.1029/2004GL021467.

Maruyama, T., Ma. Guayi, and M. Nakamura (2004), Signature of TEC storm on 6 November 2001 derived from dense GPS receiver network and ionosonde chain over Japan, *J. Geophys. Res.*, 109, A10302, doi:10.1029/2004JA010451.

Nava, B., J. Rodríguez-Zuluaga, K. Alazo-Cuartas, A. Kashcheyev, Y. Migoya-Orué, S.M. Radicella, C. Amory-Mazaudier and R. Fleury (2016), *J. Geophys. Res.*, 121(A4), 3421–3438.

Paul, A., A. Das, S.K. Chakraborty and A. DasGupta (2005), Estimation of satellite-based augmentation system grid size at low latitudes in the Indian zone, *NAVIGATION*, 2005, *52*, 15-22.

Paul, A., B. Roy, S. Ray, A. Das and A. DasGupta (2011), Characteristics of intense space weather events as observed from a low latitude station during solar minimum, *J. Geophys. Res.*, 116, A10307, doi:10.1029/2010JA016330.

Prolls, G.W., L.H. Brace, H.G. Mayr, G.R. Carignan, T.L. Killeen and J.A. Klobuchar (1991), Ionospheric Storm Effects at Subauroral Latitudes: **A** Case Study, *J. Geohys. Res.*, **96,** *A2*, 1275-1288.

Ray, S., A. DasGupta, A. Paul and P. Banerjee (2003), Estimation of Minimum Separation of Geostationary Satellites for Satellite-Based Augmentation System (SBAS) from Equatorial Ionospheric Scintillation Observations, *The Journal of Navigation*, 56, 137–142.

Ray, S., B. Roy, and A. Das (2015), Occurrence of equatorial spread F during intense geomagnetic storms, *Radio Sci.*, 50, doi:10.1002/2014RS005422.

Richmond, A. D., C. Peymirat, and R. G. Roble (2003), Long-lasting disturbances in the equatorial ionospheric electric field simulated with a coupled magnetosphere-ionosphere-thermosphere model, *J. Geophys. Res.*, 108(A3), 1118, doi:10.1029/2002JA009758.

Roy, B., and A. Paul (2013), Impact of space weather events on satellite-based navigation, *Space Weather, 11,* 680-686, doi: 10.1002/2013SW001001.

Sastri, J. H., M. A. Abdu, I. S. Batista, and J. H. A. Sobral (1997), Onset conditions of equatorial (range) spread F at Fortaleza, Brazil, during the June solstice, *J. Geophys. Res.*, 102(A11), 24,013– 24,021.

Stoneback, R. A., R. A. Heelis, R. G. Caton, Y.-J. Su, and K. M. Groves (2013), In situ irregularity identification and scintillation estimation using wavelets and CINDI on C/NOFS, *Radio Sci.*, *48*, 388–395, doi:10.1002/rds.20050.

Tsurutani, B., A. Mannucci, and B. Ijima, et al. (2004), Global dayside ionospheric uplift and enhancement associated with interplanetary electric fields, *J. Geophys. Res.*, 109, A08302, doi:10.1029/2003JA010342.

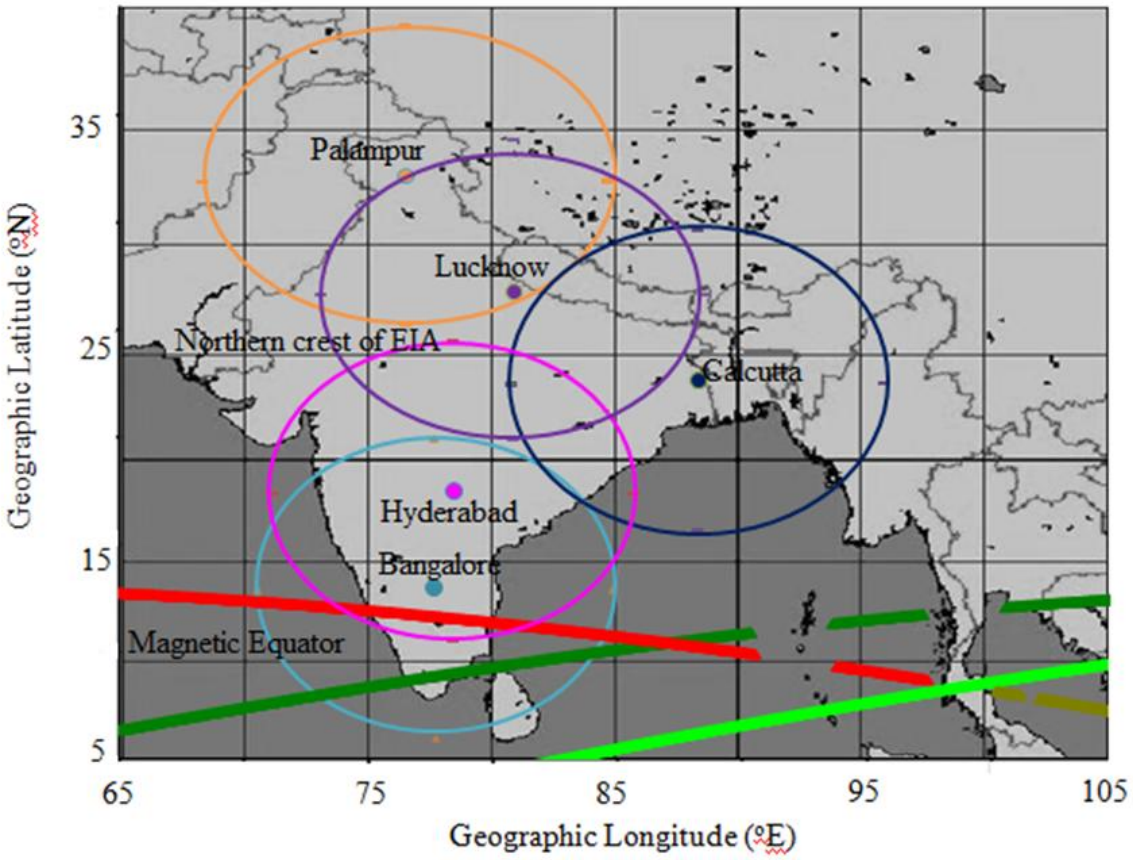

Figure 1: Locations of the stations Bangalore, Hyderabad, Calcutta, Lucknow and Palampur on a map of India. Zone of reception of satellite signals from these stations above an elevation of 15° are shown by the different colored ellipses. The magnetic equator and the typical location of the northern crest of the Equatorial Ionization Anomaly (EIA) are indicated in the map. The tracks of C/NOFS satellites that exhibited fluctuations in total ion density and intercepted the Indian longitude sector have been shown with different shades of green in Figure 1. The portions of the tracks with fluctuations have been marked with red.

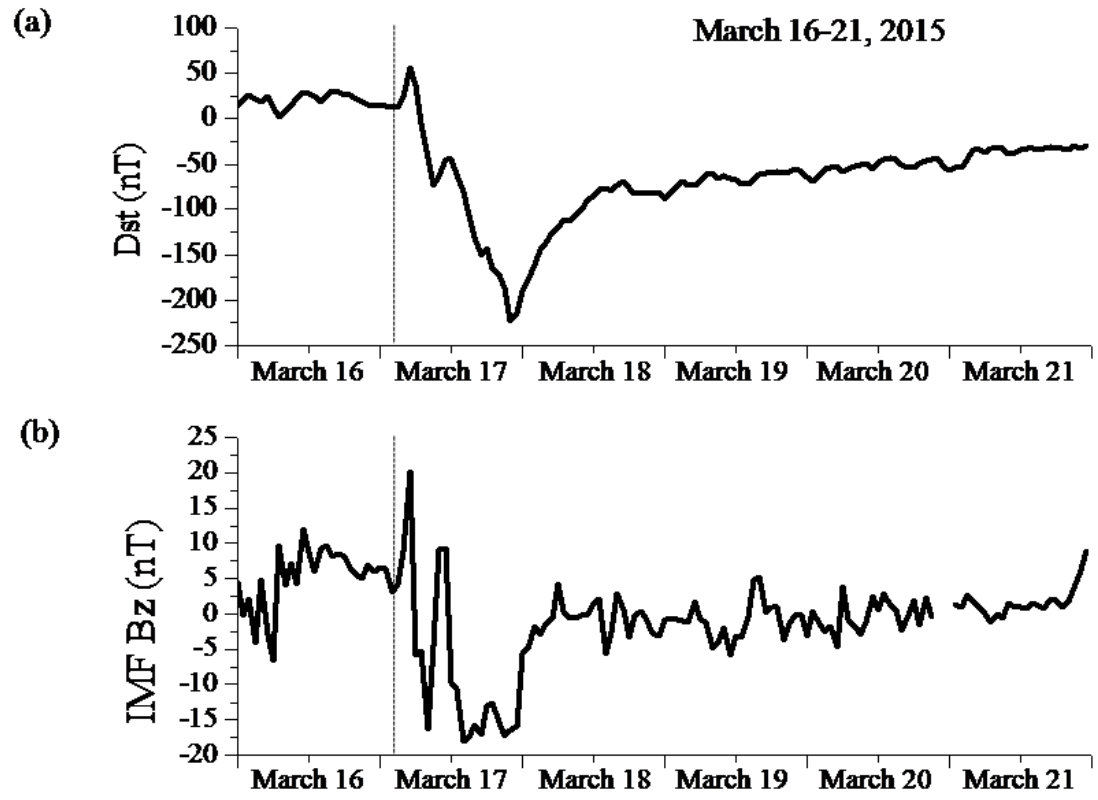

Figure 2: Variation of the (a) Dst index and (b) IMF Bz during March 16-22, 2015. The dotted lines show the time of storm commencement in each plot.

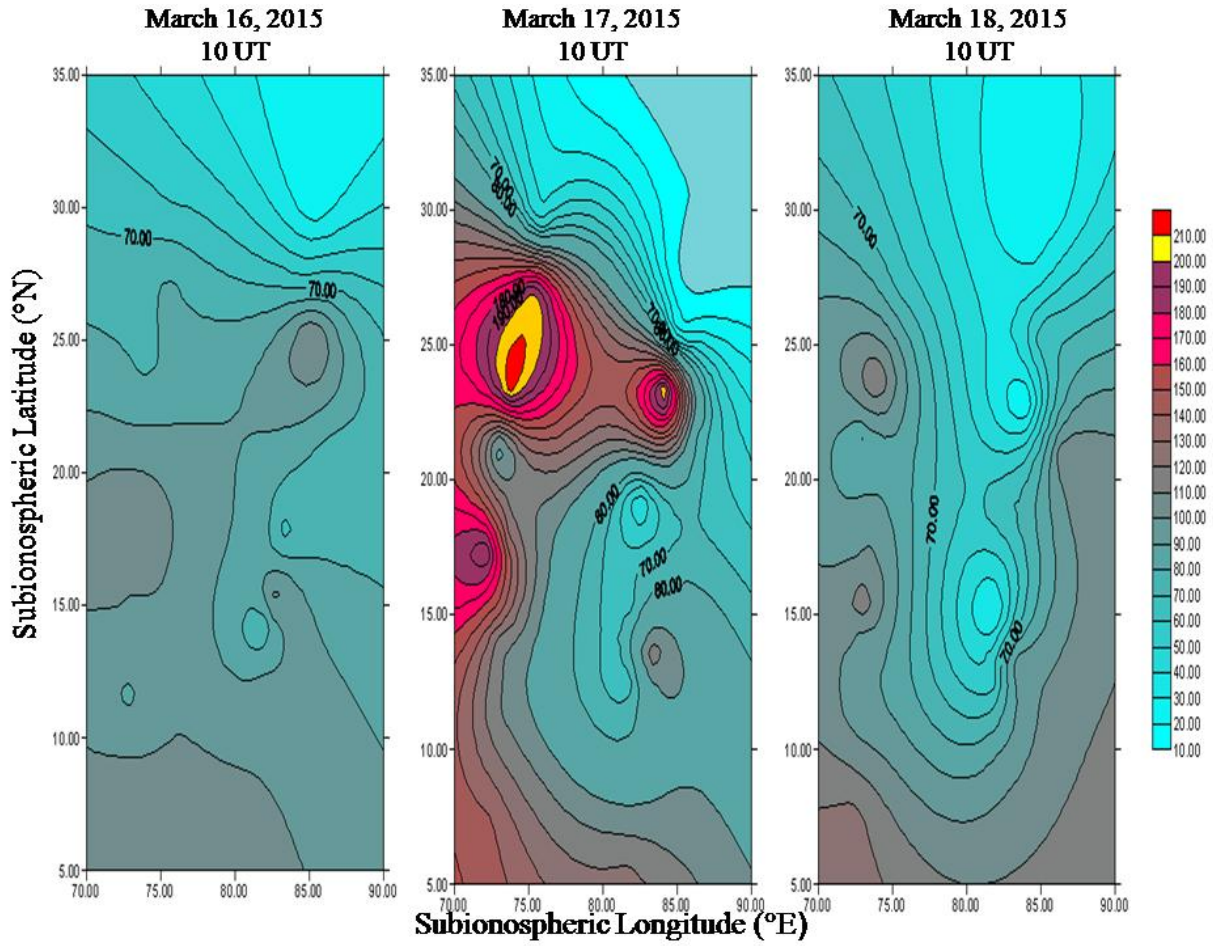

Figure 3: Slant TEC maps generated using GPS data recorded at Bangalore, Hyderabad, Lucknow and Palampur, as a function of subionospheric latitude and longitude, at 10UT on March 16, 17 and 18, 2015

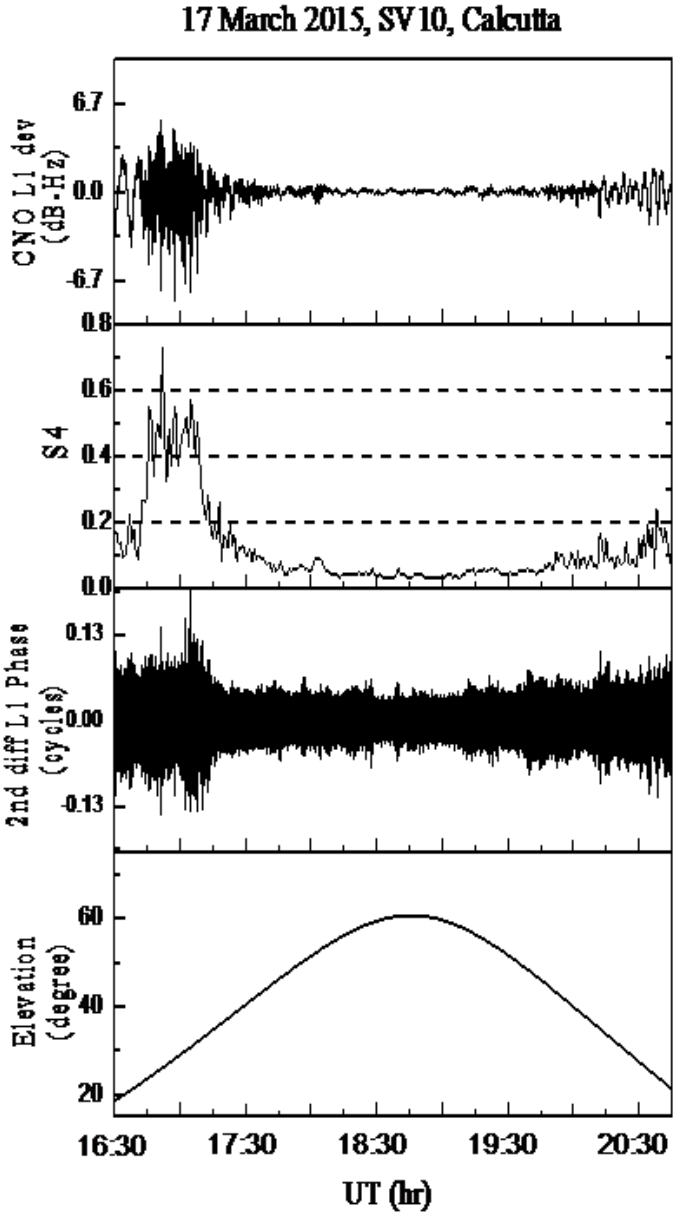

Figure 4: CNO deviations for scintillations observed from Calcutta on SV10, S4, second difference of phase and satellite elevation angle variations during 16:30-20:45UT of March 17, 2015

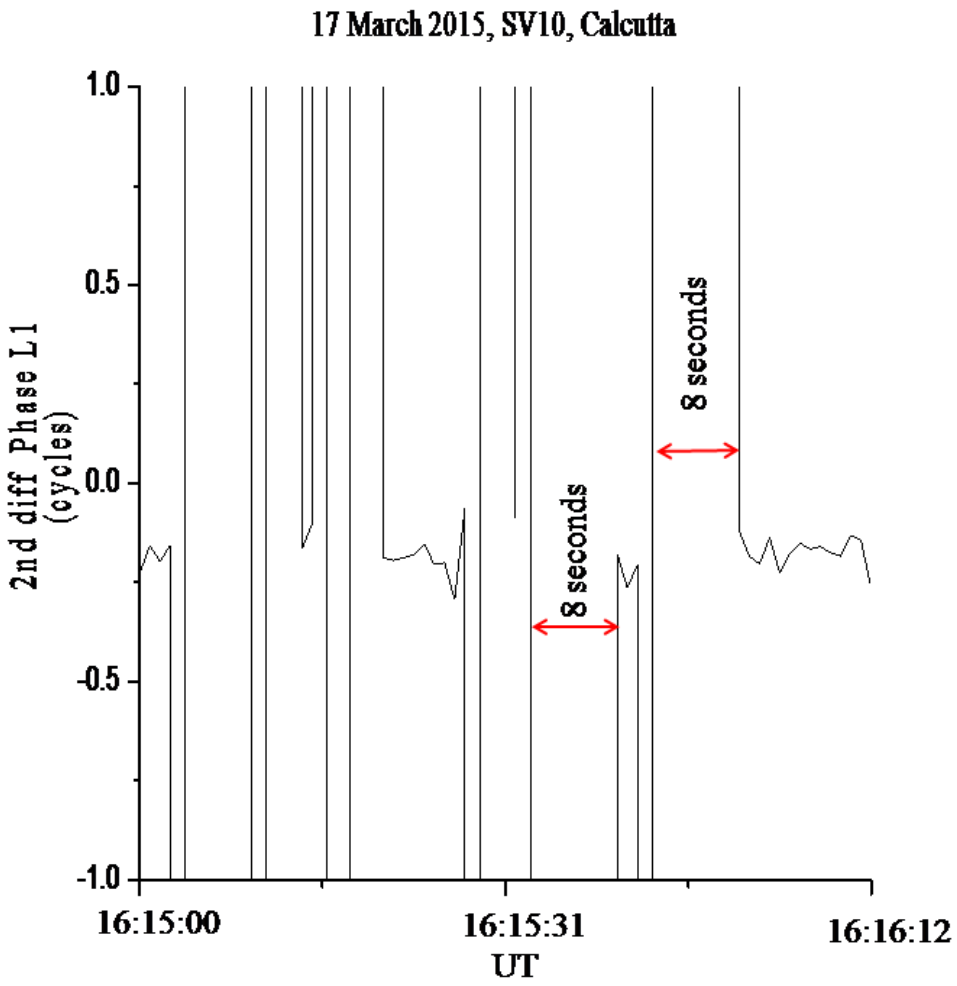

Figure 5: Second difference of the recorded phase on the GPS SV10 L1 signal over a brief interval 16:15-16:16UT to show occurrence of cycle slips. Discontinuities in phase of duration 8s could be found after 16:15:31UT on the SV10 link indicating occurrence of cycle slips

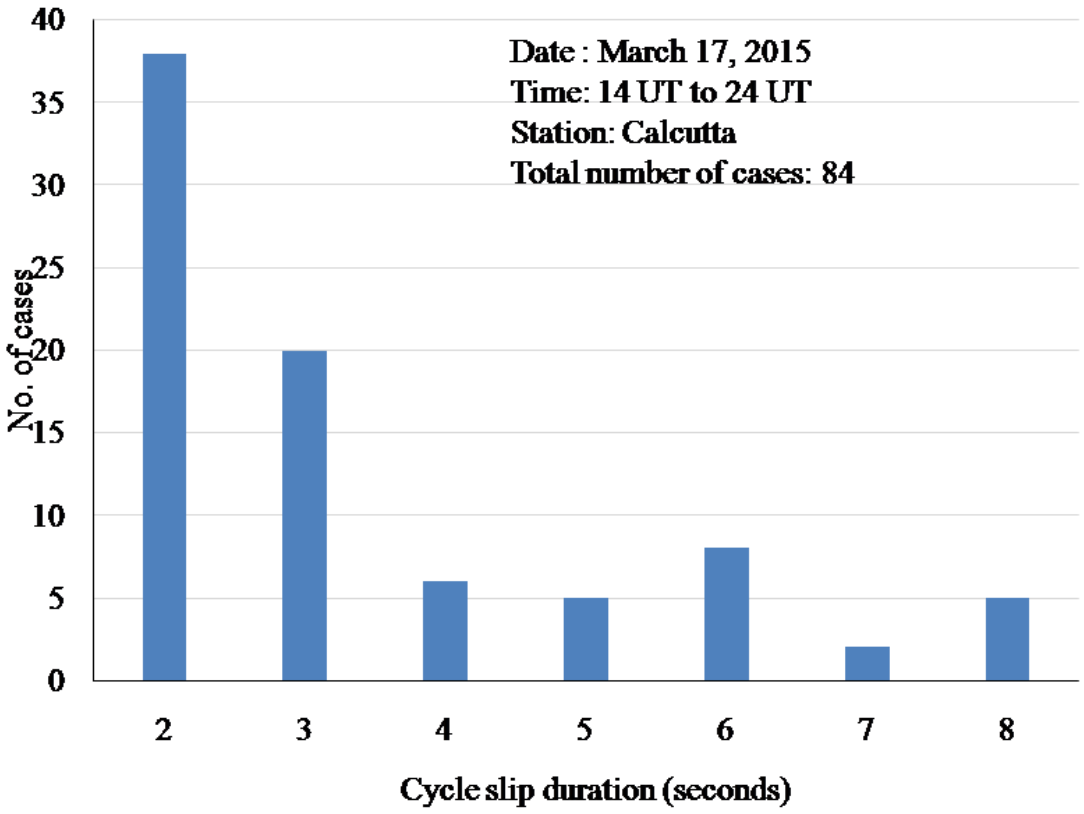

Figure 6: Statistics of cycle slips of different durations observed on different GPS links from Calcutta on March 17, 2015

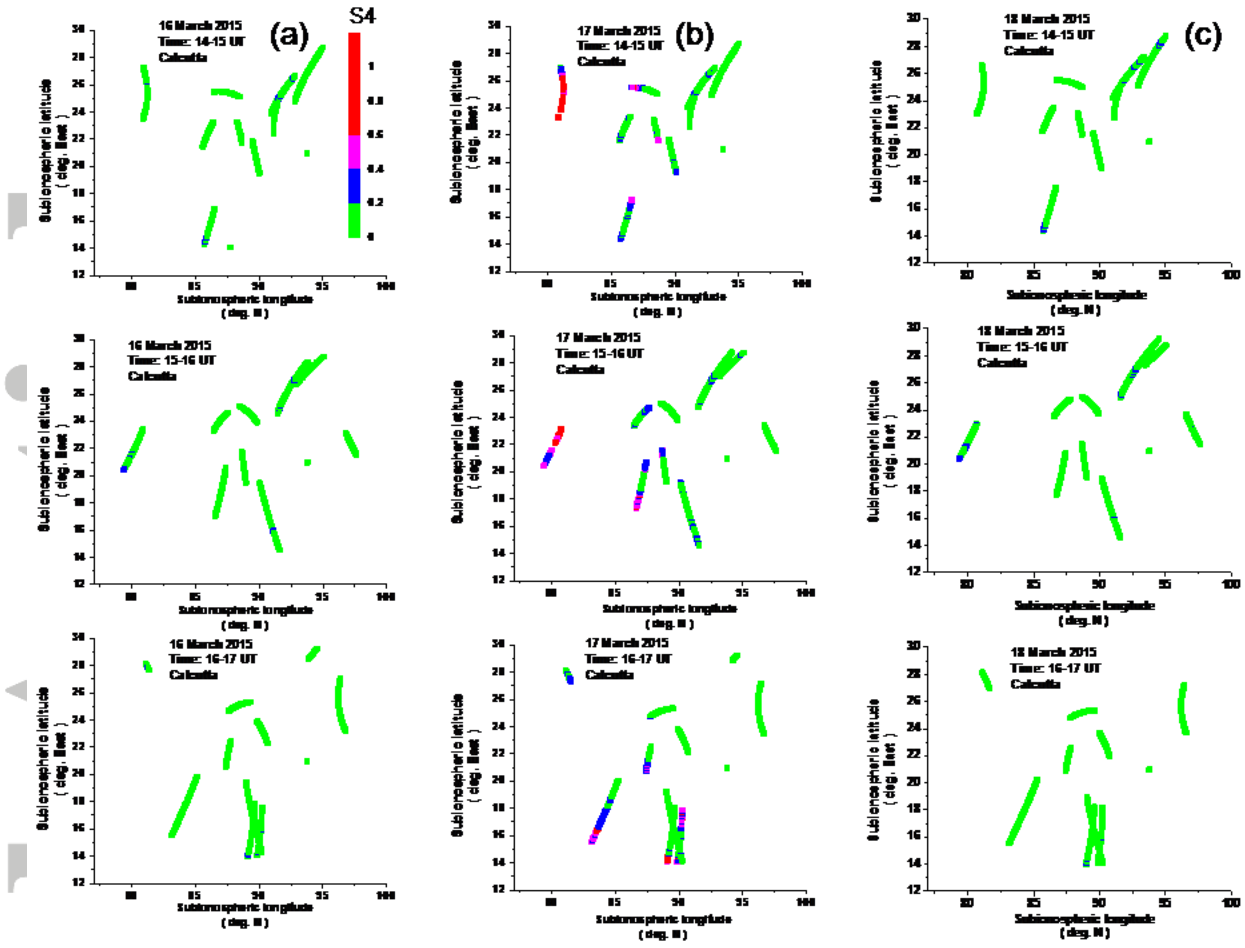

Figure 7: Observation of scintillations from Calcutta on different GPS tracks for each hour of 14:00-17:00UT of (a) March 16, (b) March 17 and (c) March18, 2015. The GPS tracks are plotted in terms of subionospheric latitude and longitude and color indexed for different S4 levels

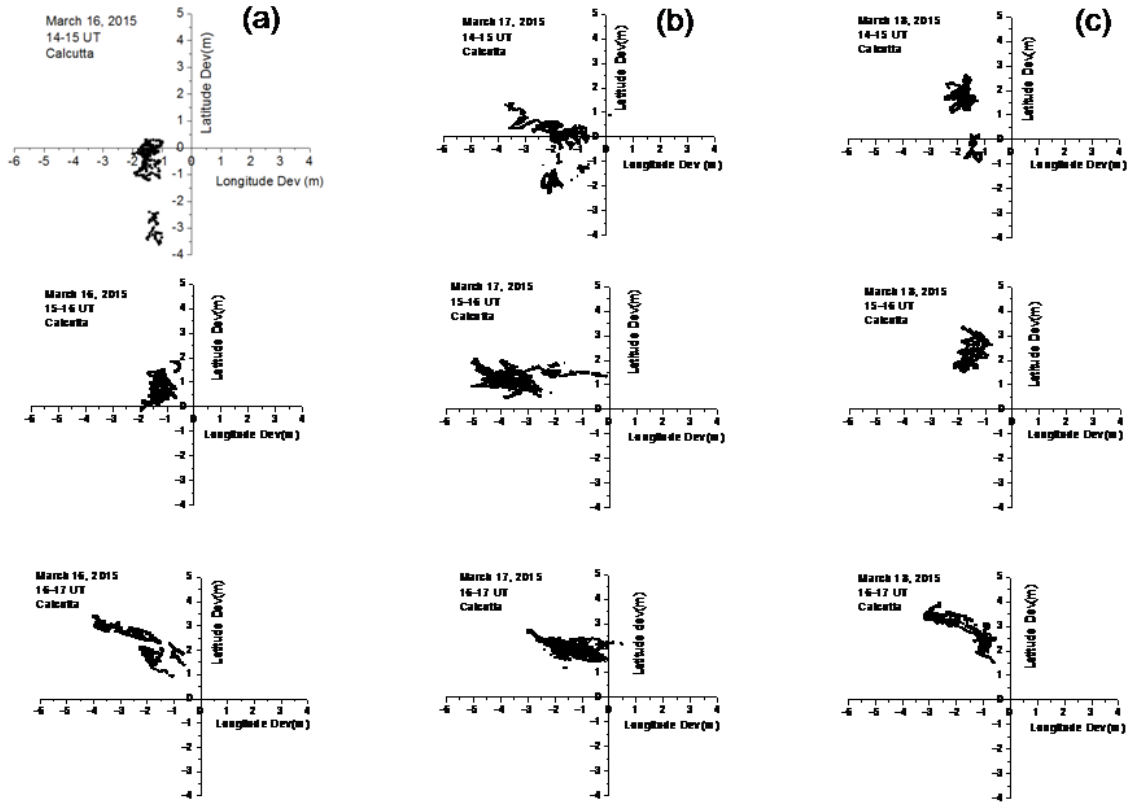

Figure 8: Position deviations of the receiver measured at Calcutta, for each hour of 14:00-17:00UT of March 16, 17 and18, 2015. The position deviations, expressed in terms of latitude and longitude in meters, have been calculated taking the reference at 00:00UT

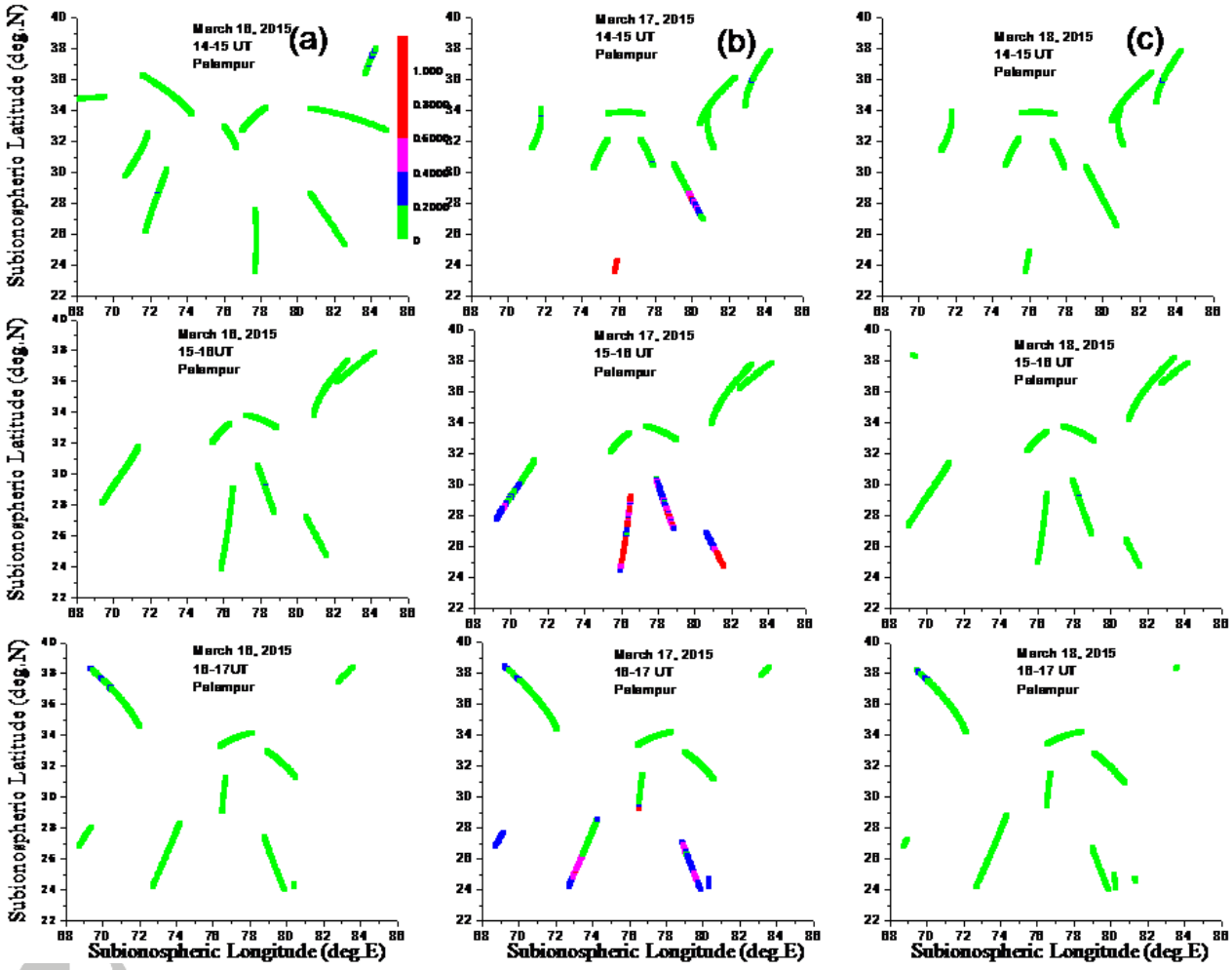

Figure 9: Observation of scintillations from Palampur on different GPS tracks for each hour of 14:00-17:00UT of (a) March 16, (b) March 17, and (c) March18, 2015. The GPS tracks are plotted in terms of subionospheric latitude and longitude and color indexed for different S4 levels

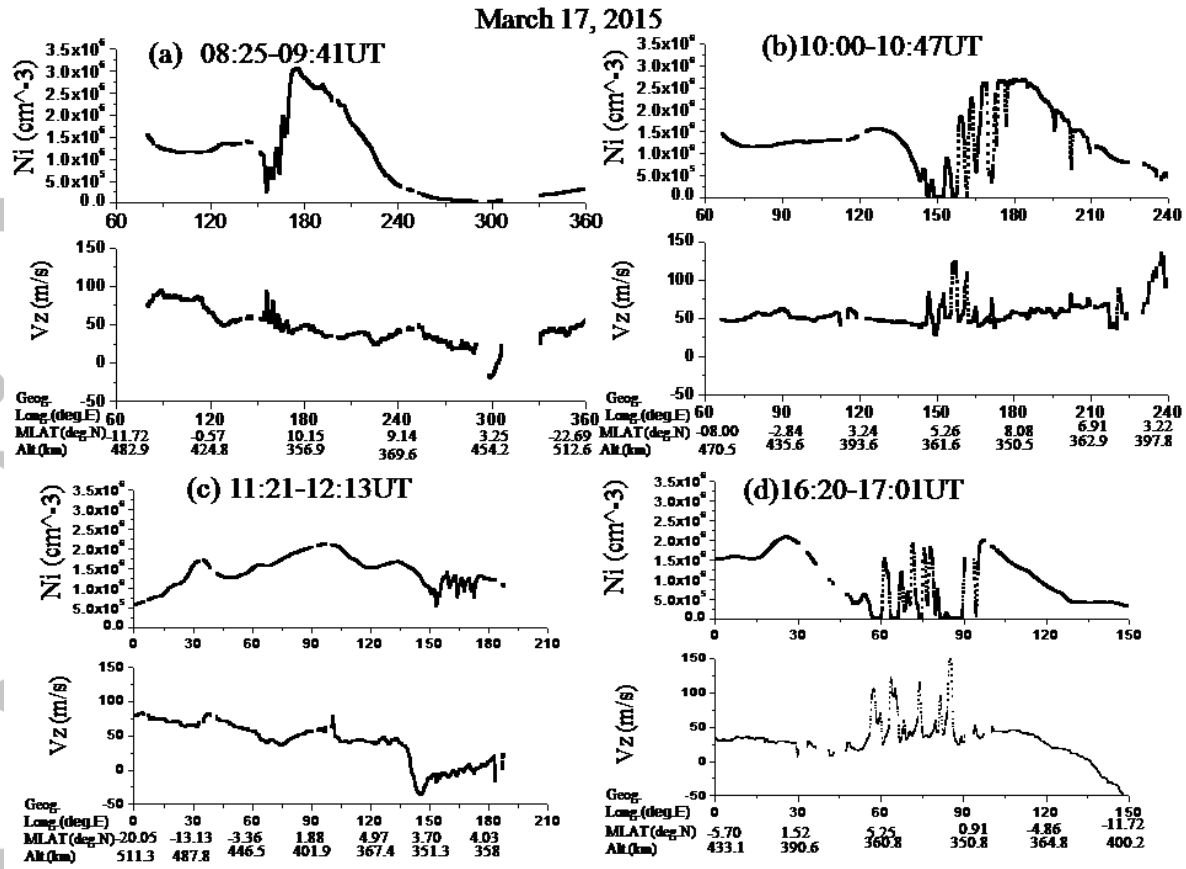

Figure 10: Variation of the total ion density and vertical upward velocity (Vz) of the F-region measured by C/NOFS over the magnetic equator in the (a) East Pacific longitude sector (150^{o}E-180^{o}E) during 08:25-09:41UT (b) East Pacific longitude sector (150^{o}E-180^{o}E) during 10:00-10:47UT (c) East Pacific longitude sector (150^{o}E-180^{o}E) during 11:21-12:13UT and (d) Indian longitude sector (60^{o}E-90^{o}E) during 16:20-17:01UT.